Available online at www.sciencedirect.com

ScienceDirect

journal homepage: www.jfda-online.com

Original Article

Fabrication of a novel electrochemical sensor for determination of hydrogen peroxide in different fruit juice samples

Navid Nasirizadeh [a,*], Zahra Shekari [a], Ali Nazari [c], Masoumeh Tabatabaee [b]

[a] Scientific Society of Nanotechnology, Yazd Branch, Islamic Azad University, Yazd, Iran
[b] Department of Chemistry, Yazd Branch, Islamic Azad University, Yazd, Iran
[c] Department of Art and Architectural, Yazd Branch, Islamic Azad University, Yazd, Iran

ARTICLE INFO

Article history:
Received 19 February 2015
Received in revised form
30 May 2015
Accepted 15 June 2015
Available online 26 July 2015

Keywords:
amperometry
electroreduction
hydrogen peroxide
reactive blue 19

ABSTRACT

A new hydrogen peroxide (H_2O_2) sensor is fabricated based on a multiwalled carbon nanotube-modified glassy carbon electrode (MWCNT-GCE) and reactive blue 19 (RB). The charge transfer coefficient, α, and the charge transfer rate constant, k_s, of RB adsorbed on MWCNT-GCE were calculated and found to be 0.44 ± 0.01 Hz and 1.9 ± 0.05 Hz, respectively. The catalysis of the electroreduction of H_2O_2 by RB-MWCNT-GCE is described. The RB-MWCNT-GCE shows a dramatic increase in the peak current and a decrease in the overvoltage of H_2O_2 electroreduction in comparison with that seen at an RB modified GCE, MWCNT modified GCE, and activated GCE. The kinetic parameters such as α and the heterogeneous rate constant, k', for the reduction of H_2O_2 at RB-MWCNT-GCE surface were determined using cyclic voltammetry. The detection limit of 0.27μM and three linear calibration ranges were obtained for H_2O_2 determination at the RB-MWCNT-GCE surface using an amperometry method. In addition, using the newly developed sensor, H_2O_2 was determined in real samples with satisfactory results.

1. Introduction

Hydrogen peroxide (H_2O_2) is an essential mediator used in many fields of practice such as food, pharmaceutical, clinical, diagnostic, environmental protection, and in industries [1]. Indeed, H_2O_2 has wide applications in industrial processes as a universal oxidant and is a very important intermediate agent in environmental and biological reactions. It has also emerged as an important by-product of enzymatic reactions in biosensing processes, because it is released during the oxidation of substrates in the presence of oxygen [2,3]. Monitoring H_2O_2 with a reliable, rapid, and economical method is of great significance for numerous

* Corresponding author.
E-mail address: nasirizadeh@iauyazd.ac.ir (N. Nasirizadeh).
http://dx.doi.org/10.1016/j.jfda.2015.06.006

processes. The determination of H_2O_2 has been an important project over the past century. This is still something to accomplish, especially with the recent realizations about the existence of H_2O_2 in environmental samples. Various techniques including fluorimetry [4], titrimetry [5], chemiluminescence [6], spectrophotometry [7], photometry [8], and electrochemistry [9–11] have been developed for this purpose. Among these techniques, electrochemistry based on simple and low-cost electrodes has been extensively used to determine H_2O_2 [12]. It has been a preferred technique due to its quick response, low cost, simple instrumentation, high sensitivity, and possibility of miniaturization [13]. A number of enzyme electrodes reported for H_2O_2 determination are used due to their simplicity, high sensitivity, and selectivity [14]. Although, many enzymatic H_2O_2 assays possess good sensitivity and selectivity, native enzymes gradually lose their catalytic activity after repeated measurements and they are comparatively expensive. Therefore, the development of enzyme-free H_2O_2 sensors with a low detection limit and a wide responding range is preferred. However, the direct electrochemistry of H_2O_2 requires a higher over-potential and slow electrode kinetics on many electrode materials. Electrodes modified with different electroactive materials have the ability to detect H_2O_2 at low potentials. In recent years, various kinds of electrochemical sensors based on detection of different compounds in the food industry have been developed [15–18]. The study of electrochemical biosensors has been in progress to improve the speed, selectivity, sensitivity, and cost of producing chemical compounds. Immobilization of mediators in charge of electron transfer to electrode surfaces is a key step for the design, fabrication, and performance of sensors and biosensors [19]. Quinones are excellent electron mediators that efficiently reduce the working potentials and eliminate the effects of various electroactive substances in real samples; they have been successfully used in numerous biosensors to detect H_2O_2 [20,21]. Reactive blue 19 (RB) is a derivative of quinone (see its structure in Scheme 1). Owing to the good reactivity of quinone derivative mediators, it seems that the use of RB as a modifier could be important to yield some new information about the catalyzation of slow reactions. In this work, for the first time, RB is introduced as a catalytic compound for electroreduction of H_2O_2, then its electrochemical behavior and kinetic parameters are investigated. Cyclic voltammetry and amperometry were used to investigate the electrochemical properties and electrocatalytic activity of the modified electrode for determination of H_2O_2.

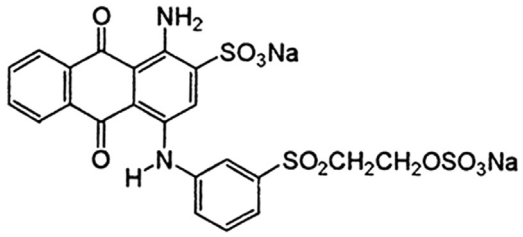

Scheme 1 – Structure of reactive blue 19.

2. Methods

2.1. Reagents and apparatus

H_2O_2, dimethyl formamide, and the other chemicals used to produce the buffer solution were obtained from Merck Company (Darmstadt, Germany) and used as received. RB was obtained from Sigma–Aldrich (St Louis, MO, USA). Multiwalled carbon nanotubes (MWCNTs; with a diameter of 10–20 nm, length of 5–20 μm, and purity of 95%) were purchased from NanoLab Inc. (Waltham, MA, USA). All chemical reagents were of analytical grade. Phosphate buffer solutions (0.1M) were prepared with H_3PO_4, the pH was adjusted with 2.0M NaOH. All solutions were prepared with doubly distilled water.

Electrochemical experiments were carried out with an Autolab modular electrochemical system (ECO Chemie, Utrecht, The Netherlands) equipped with a PGSTA 30 module and driven by GPES 4.9 software, in conjunction with a three-electrode cell. The cell used was equipped with an RB-MWCNT-modified glassy carbon electrode (GCE) as a working electrode, a platinum electrode (Azar Electrode Co, Tabriz, Iran) as an auxiliary electrode, and a saturated calomel electrode as a reference electrode. All potentials in the text are quoted versus this reference electrode. The pH was measured with a pH/mV meter model 827 (Metrohm, Riverview, FL, USA).

2.2. Preparation of modified electrodes

The procedure of fabricating various modified electrodes was as follows. Prior to modification, a bare GCE was polished successively with 0.05 μm Al_2O_3 slurry on a polishing cloth and then rinsed with doubly distilled water. To be electrochemically activated, the cleaned electrode was immersed in a 0.1M sodium bicarbonate solution and activated by a continuous potential cycling from −1.45 to 1.7 V at a sweep rate of 100 mV/s. To prepare a RB modified GCE (RB-GCE) the activated GCE (AGCE) was rinsed and placed in a 0.10mM solution of RB in a 0.1M phosphate buffer (pH 7.0). It was modified by eight cycles of potential sweep between −0.4 and 0.5 V at 20 mV/s. To fabricate MWCNT-GCE, 3 μL of dimethyl formamide-MWCNT solution (1 mg/mL) was placed directly onto the AGCE surface and dried at room temperature for 30 minutes to form a MWCNT film at the GCE surface. An RB-MWCNT-GCE was prepared by immersing the MWCNT-GCE in a 0.10mM solution of RB in a 0.1M phosphate buffer (pH 7.0; Scheme 2). It was modified using the same procedure as for RB-GCE.

3. Results and Discussion

3.1. Electrochemical behavior of RB-MWCNT-GCE

In recent years, the mechanism of electrodeposition of *o*- or *p*-hydroquinone derivatives, as modifiers, on the surface of an activated GCE has been a matter for discussion [22–25]. Fig. 1 shows the cyclic voltammograms of the

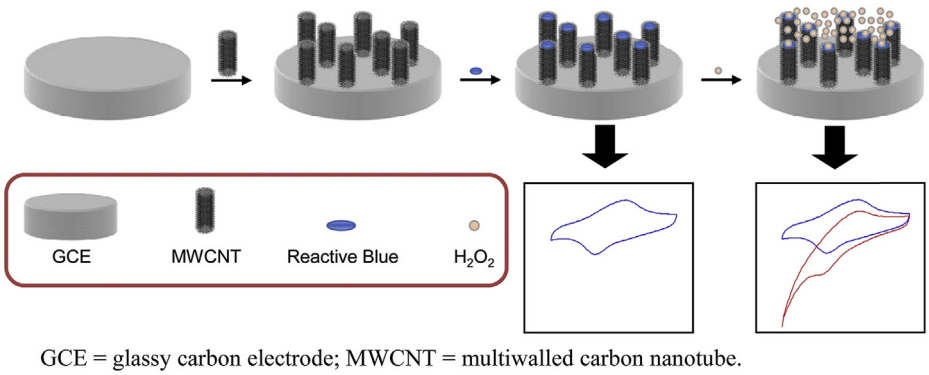

GCE = glassy carbon electrode; MWCNT = multiwalled carbon nanotube.

Scheme 2 – Schematic diagram for the sensor fabrication and determination of H_2O_2. GCE = glassy carbon electrode; MWCNT = multiwalled carbon nanotube.

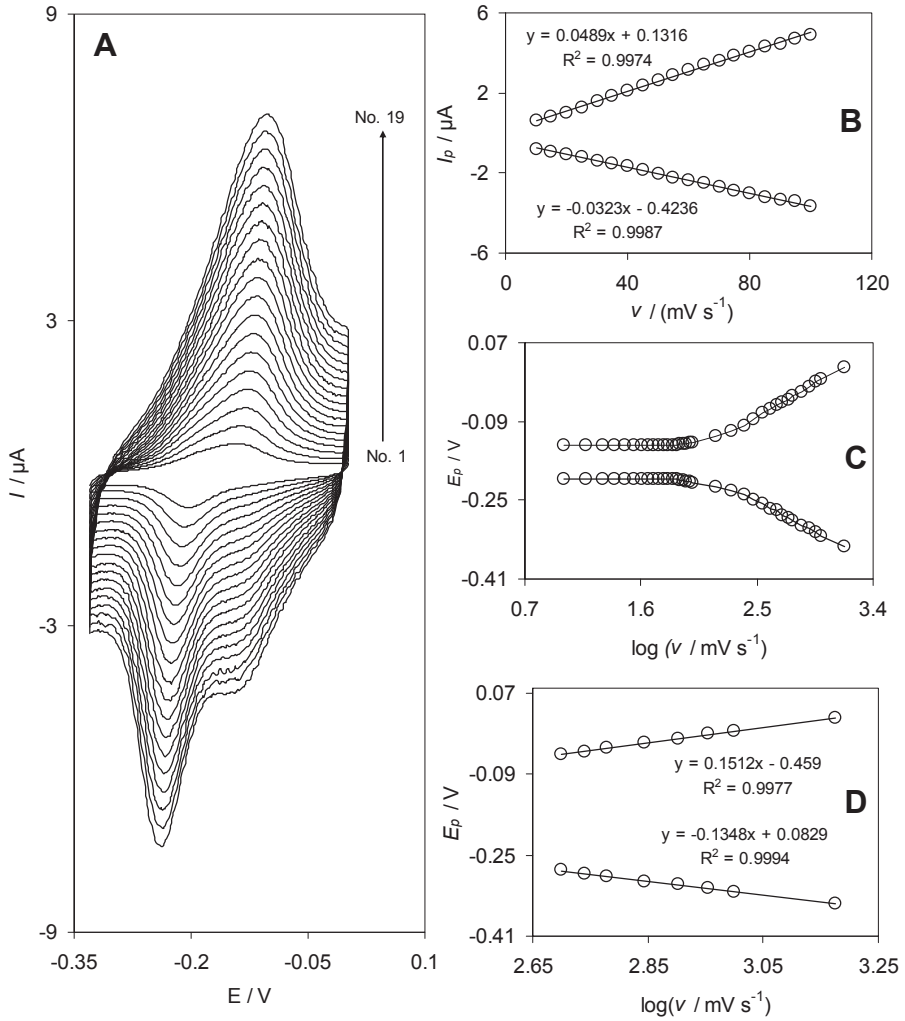

Fig. 1 – (A) Cyclic voltammograms of the reactive blue 19 multiwalled carbon nanotube-modified glassy carbon electrode in 0.1M phosphate buffer solution (pH 7.0) at different scan rates. The numbers 1–19 correspond to 15 mV/s, 20 mV/s, 25 mV/s, 30 mV/s, 35 mV/s, 40 mV/s, 45 mV/s, 50 mV/s, 55 mV/s, 60 mV/s, 65 mV/s, 70 mV/s, 75 mV/s, 80 mV/s, 85 mV/s, 90 mV/s, 95 mV/s, and 100 mV/s, respectively. (B) Plots of anodic and cathodic peak currents vs. the scan rate. (C) Variation of the peak potentials vs. the logarithm of the scan rate. (D) Magnification of the plot inset B for high scan rates.

Table 1 – Variations in anodic peak surface coverage, Γ, as a function of reactive blue 19 (RB) modified glassy carbon electrode multiwalled carbon nanotube (MWCNT) amounts, RB solution pH, RB solution concentration, [RB], potential scan rates, v, and number of cycles of potential scans, number of cycles, during the modification step. In all case the scan rate was 20 mV/s and the surface coverage is in 10^{-11} mol/cm.

MWCNT amount (mg/cm^3)	Γ	pH	Γ	[RB] (mM)	Γ	v (mV/s)	Γ	No. of cycles	Γ
0.2	6.8	3	8.5	0.2	2.1	10	12.9	2	13.3
0.4	8.2	4	9.6	0.4	6.4	15	13.4	4	14.5
0.6	9.5	5	10.2	0.6	10.7	20	15.5	6	15.2
0.8	10.6	6	11.1	0.8	12.6	30	10.7	8	16.1
1.0	11.4	7	12.5	1.0	14.1	40	9.6	10	15.8
1.2	11.4	8	9.8	1.2	13.9	50	6.2	12	15.5
1.4	11.2	9	6.9	1.4	14.0	60	4.9	14	15.7

RB-MWCNT-GCE in a 0.1M phosphate buffer solution (pH 7.0) at various potential scan rates. The plots of the anodic and cathodic peak currents versus the scan rate exhibit a linear relation (Fig. 1, inset B) as predicted theoretically for a surface-immobilized redox couple. This indicates the limitation arising from charge transfer kinetics. In other words, this is the range in which the reaction appears as quasireversible [26].

When the potential was scanned between −330 and 0 mV, a surface-immobilized redox couple with a conditional formal potential, $E^{0'}$, of −173 mV was observed. In addition, $E^{0'}$ was almost independent of any potential scan rate for sweep rates ranging from 10 mV/s to 100 mV/s, suggesting facile charge transfer kinetics over this range of sweep rates. According to the method described by Laviron [27], the charge transfer coefficient, α, and the apparent heterogeneous charge transfer rate constant, k_s, for the electron transfer between an MWCNT-GCE and a surface confined redox couple of RB can be evaluated in cyclic voltammetry by the variation of the anodic and cathodic peak potentials with the logarithm of scan rates.

For high scan rates, this theory predicts a linear dependence of E_p upon $\log v$, which can be used to extract the kinetic parameters of α and k_s from the slope and intercept of such

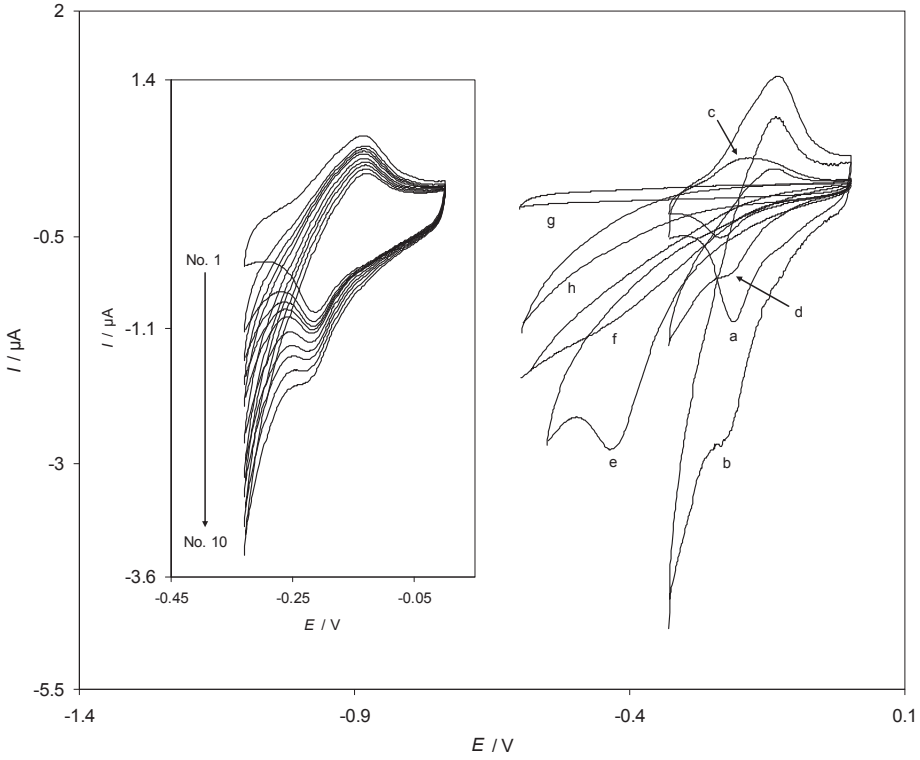

Fig. 2 – Cyclic voltammograms of different electrodes in a 0.1M phosphate buffer (pH 7.0) solution in the absence (a, c, g) and presence (b, d, e, f, h) of 0.40mM H_2O_2: (a, b) reactive blue 19 multiwalled carbon nanotube-modified glassy carbon electrode (RB-MWCNT-GCE), (c, d) RB-GCE, (e) MWCNT-GCE, (f) acquired GCE and (g, h) BGCE. Inset shows the dependence of cyclic voltammetric response at a RB-MWCNT-GCE on H_2O_2 concentration in 0.1M phosphate buffer (pH 7). The numbers of 1–10 correspond to 0.0–473.7μM H_2O_2. In all cases the scan rate was 20 mV/s.

Table 2 – Comparison of electrocatalytic reduction of H_2O_2 (0.40mM) on various electrode surfaces at pH 7.0.

Name of electrode	Reduction potential (mV)	Reduction current (μA)
MWCNT-GCE	−431	−1.353
RB-GCE	−221	−0.397
RB-MWCNT-GCE	−215	−1.73

MWCNT-GCE = multiwalled carbon nanotube-modified glassy carbon electrode; RB–GCE = reactive blue modified glassy carbon electrode; RB-MWCNT-GCE = reactive blue multi–walled carbon nanotube-modified glassy carbon electrode.

plots respectively. The results indicate that the values of the peak potentials were proportional to the logarithms of scan rates higher than 500 mV/s (Fig. 1C). Using these plots at pH 7.0, the value of $\alpha = 0.44 \pm 0.01$ was obtained. From the values of ΔE_p corresponding to different sweep rates, an average value of k_s was found to be 1.9 ± 0.05 Hz. This value of k_s is comparable to those reported for other modifiers [21,24,27,28]. Since the electron transfer rate constant for the RB is about 1.9 Hz, it can be used as an excellent electron transfer mediator for electrocatalytic processes.

The effects of different experimental variables in the immobilization of RB were investigated to optimize the testing performance. In other words, the effects of the MWCNT amounts, the modifier solution pH, its concentration, the potential scan rate, and the number of potential recyclings were examined on the performance of modified electrode, and the anodic surface coverage was used as a measure of the surface deposited RB. The surface coverage (Γ) of the modified electrode was determined from the following equation, $\Gamma = Q/nFA$, where Q is the charge obtained by integrating the anodic or cathodic peak under the background correction and other symbols have their usual meanings, assuming an n value of 2. Table 1 illustrates the effect of different experimental conditions involved in the fabrication of RB-MWCNT-GCE. However, assuming that no interaction can exist between the variables, the one-at-a- time procedure [29] was used for optimization. The results in Table 1 show that the best surface coverage was obtained when the modification was carried out in a 1.0 mM RB solution with pH 7.0 (0.1M phosphate buffer) and the potential scan rate, was 20 mV/s.

Moreover, the intraday repeatability of RB-MWCNT-GCE was tested by 10 replicate measurements in the buffer solution (pH = 7). The decrease of current signal was about 5%. Also, the long-term stability of RB-MWCNT-GCE was measured for 3 days. When cyclic voltammograms were recorded after the modified electrode was stored in at room

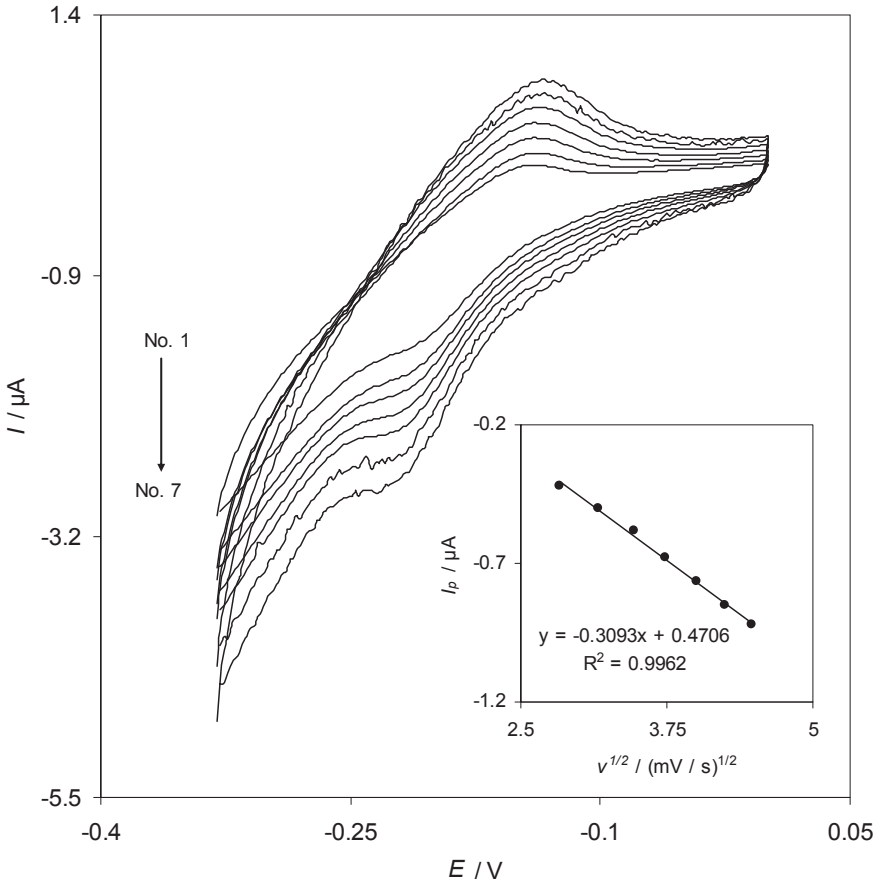

Fig. 3 – Cyclic voltamograms of reactive blue 19 multiwalled carbon nanotube-modified glassy carbon electrode in 0.1M phosphate buffer (pH 7.0) containing 0.40mM H_2O_2 at different scan rates. The numbers of 1–7 correspond to scan rates of 8 mV/s, 10 mV/s, 12 mV/s, 14 mV/s, 16 mV/s, 18 mV/s, and 20 mV/s. Inset: variation of the electrocatalytic peak current (I_p) versus the square root of sweep rate.

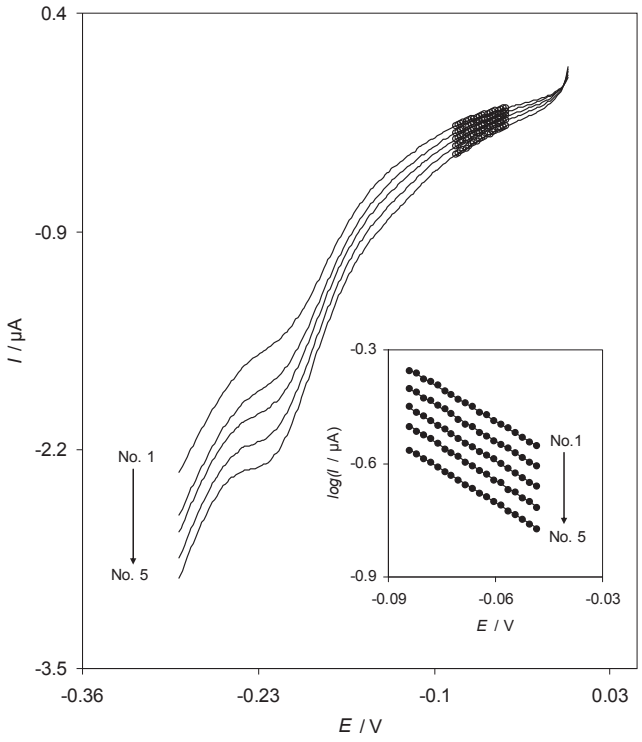

Fig. 4 – Linear sweep voltammogram of reactive blue 19 multiwalled carbon nanotube-modified glassy carbon electrode in 0.1M phosphate buffer solution (pH 7.0) containing 0.40 mM H_2O_2 at different scan rates (8–16 mV/s). Inset shows the Tafel plots derived from the linear sweep voltammograms.

temperature, only a 7% decrease was observed in the current response of the modified electrode. The initial decay of the current response of the voltammograms observed in both cases might be due to the release of the modifiers that are weakly bonded to MWCNT deposited on the electrode surface and can be separated somewhat easily.

3.2. *Electrocatalytic reduction of H_2O_2 at RB-MWCNT-GCE*

To test the electrocatalytic activity of the produced RB-MWCNT-GCE toward H_2O_2 reduction, cyclic voltammetric responses were obtained in a phosphate buffer solution at pH 7 in the absence and presence of H_2O_2 (Fig. 2). Fig. 2 indicates the cyclic voltammograms of different electrodes in a 0.1M phosphate buffer (pH 7.0) solution in the absence (a, c, g) and presence (b, d, e, f, h) of 0.40 mM H_2O_2. Curves a and b of Fig. 2 show the cyclic voltammograms of RB-MWCNT-GCE in the absence (a) and the presence (b) of 0.4mM of H_2O_2. As expected for electrocatalytic reduction, there was an increase in the cathodic peak current of RB-MWCNT-GCE_{red}/RB-MWCNT-GCE_{ox} redox couple at the potential of −215 mV in the presence of H_2O_2, whereas the oxidation peak current virtually disappeared. This reflects the efficiency of the catalytic reaction. What occurred is basically because H_2O_2 in solution diffuses onto the electrode surface and oxidizes RB-MWCNT-GCE_{red} into RB-MWCNT-GCE_{ox}. This process increases the cathodic peak current, while the anodic peak current is less in the absence of H_2O_2. Under the same experimental conditions, the cyclic voltammograms of RB-GCE were recorded in the absence (Fig. 2, curve c) and the presence of 0.40mM of H_2O_2 (Fig. 2, curve d). Table 2 shows the electrochemical characteristics of H_2O_2 reduction at various electrode surfaces. The results point to the best electrocatalytic effect for H_2O_2 reduction observed at RB-MWCNT-GCE. As can be seen in the case of the reduction responses of H_2O_2 at RB-GCE and RB-MWCNT-GCE, there is a dramatic enhancement in the cathodic peak current at RB-MWCNT-GCE as compared to the value obtained at RB-GCE. Similarly, the peak potential of H_2O_2 reduction at RB-MWCNT-GCE (Fig. 2, curve b) is less negative compared with that at MWCNT–GCE (Fig. 2, curve e). Also, there is no peak potential observed for H_2O_2 at AGCE and Reactive Blue modified Glassy Carbon Electrode (RB-GCE) (Fig. 2, curve f, h). The above results clearly show that a combination of MWCNT and RB definitely improves the characteristics of H_2O_2 reduction. The inset of Fig. 2 shows the dependence of the voltammetric response of RB-MWCNT-GCE on H_2O_2 concentration. As can be seen, with the addition of H_2O_2, there was an increase in the cathodic current.

The cyclic voltammograms of a 0.40mM H_2O_2 solution at different sweep rates are shown in Fig. 3. The inset of Fig. 3 shows that the plot of the catalytic peak current versus the square root of the sweep rate is linear, suggesting that the reaction is diffusion limited. This is an ideal result for quantitative applications [25]. Also, the number of electrons, n, in the overall reduction reaction of H_2O_2 can be obtained from the plot of slope of I_P versus $v^{1/2}$ (inset of Fig. 3). According to the following equation for a totally irreversible diffusion controlled process:

$$I_p = 3.01 \times 10^5\, n[(1-\alpha)n_\alpha]^{1/2} A C_b D^{1/2} v^{1/2} \quad (1)$$

and considering $(1-\alpha)n_\alpha = 0.7$ (see below), $D = 2.34 \times 10^{-6}$ cm^2/s, $C_b = 4 \times 10^{-7}$ mol/cm^3, and $A = 0.0314$ cm^2, it is estimated that the total number of electrons involved in the reduction of H_2O_2 is $n = 2.02 \sim 2$. Similar values were also previously reported for the electroreduction of H_2O_2 [30–32].

The electrocatalytic reduction of H_2O_2 at the modified electrode surface can be explained according to an E_rC_i catalytic ($E_rC'_i$) mechanism. It is shown in the following equations [25]:

$$\text{Reactive blue}_{\text{(oxidized form)}} + 2H^+ + 2e^- \leftrightarrows \text{Reactive blue}_{\text{(reduced form)}} \quad E_r \ (2)$$

$$\text{Reactive blue}_{\text{(reduced form)}} + H_2O_2 + 2H^+ \rightarrow \text{Reactive blue}_{\text{(oxidized form)}} + 2H_2O \quad C'_i \ (3)$$

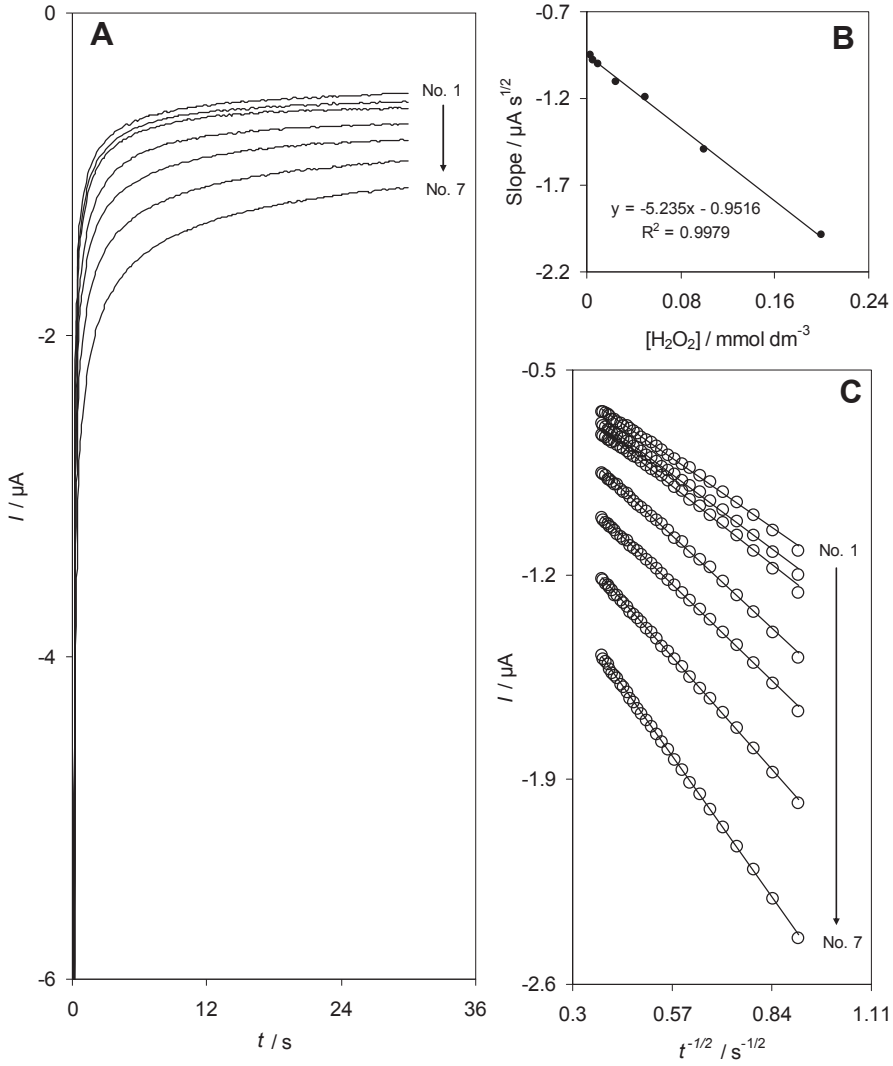

Fig. 5 – (A) Chronoamperometric responses of reactive blue 19 multiwalled carbon nanotube-modified glassy carbon electrode in a 0.1M phosphate buffer solution (pH 7.0) at a potential step −300 mV for different concentrations of H_2O_2. The numbers of 1–7 correspond to 0.003–0.20mM H_2O_2. Insets: (B) plots of *I* versus $t^{-1/2}$ obtained from chronoamperograms. (C) plot of the slope of straight lines against the H_2O_2 concentrations.

As can be seen, H_2O_2 reduces by the reduced form of RB adsorbed at the MWCNT surface, RB-MWCNT-GCE (reduced form). The symbols E_r and C_i imply reversible electrochemical and irreversible catalytic chemical reactions. For an $E_rC'_i$ mechanism, Andrieux and Saveant [33] developed a theoretical model and derived the following equation for the relationship between the electrocatalytic peak current and the concentration of the substrate for a case of a slow scan rate, υ, and a large catalytic rate constant, k':

$$I_{cat} = 0.496nFAC_bD^{1/2}\nu^{1/2}(nF/RT)^{1/2} \quad (4)$$

where D and C_b are the diffusion coefficient (2.34×10^{-6} cm^2/s is obtained by chronoamperometry as below) and the bulk concentration of H_2O_2. Low values of k' result in coefficient values lower than 0.496 [33]. For low scan rates (8–20 mV/s), we found the value of this coefficient to be 0.3 for the modified electrode based on the slope of the plot in the inset of Fig. 3. An average value of $k' = 4.6\ (\pm 0.1) \times 10^{-4}$ cm/s was calculated by such a working curve.

In order to obtain information about the rate-determining step, the linear sweep voltammograms of 0.40mM H_2O_2 were obtained at different sweep rates (Fig. 4). The inset of Fig. 4 shows the Tafel plots drawn from the data of the rising part of the current voltage curves recorded at various scan rates. This part of the voltammogram, known as Tafel region, is affected by the electron transfer kinetics between H_2O_2 and the surface-confined RB-MWCNT-GCE. The results of polarization studies for electroreduction of H_2O_2 at the modified electrode show that the average of Tafel slope of different plots agree well with the involvement of one-electron transfer process, assuming an average charge transfer coefficient of, $\alpha_{ave} = 0.3 \pm 0.01$. Also, the exchange current density, j_0, is accessible from the intercept of the Tafel plots and the geometric area.

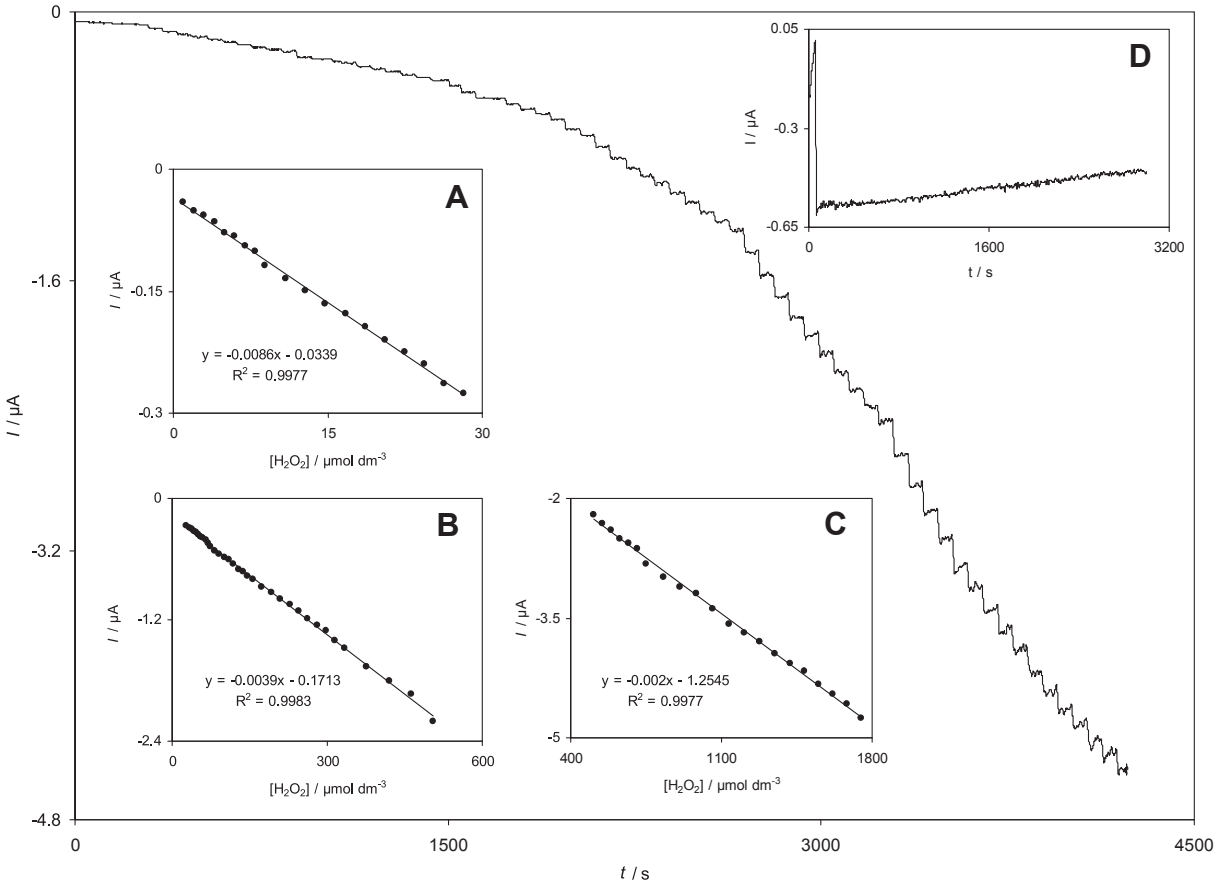

Fig. 6 – Amperometric responses at a rotating reactive blue 19 multiwalled carbon nanotube-modified glassy carbon electrode (rotation speed 2000 rpm) held at −300 mV in different concentrations of H_2O_2. Insets A, B, and C indicate variations of the amperometric currents vs. H_2O_2 concentrations in the ranges of (A) 1.99–28.2μM, (B) 282–504μM, and (C) 0.504–1.75μM. Inset D shows the stability of the response of the reactive blue 19 multiwalled carbon nanotube-modified glassy carbon electrode to 100.0μM H_2O_2 during 2900 seconds.

The average valve obtained for the exchange current density of H_2O_2 at RB-MWCNT-GCE was found to be 3.64 ± 0.1 μA/cm^2.

The electrocatalytic reduction of H_2O_2 by RB-MWCNT-GCE was also studied by chronoamperometry. The chronoamperograms obtained at the potential step of −300 mV are shown in Fig. 5. Inset A of Fig. 5 shows the experimental plots I versus $t^{-1/2}$ with the best fits for different concentrations of H_2O_2. The slopes of the resulting straight lines were then plotted versus the H_2O_2 concentration (Fig. 5,

Table 3 – Comparison of analytical parameters of several modified electrodes for H_2O_2 determination.

Modifier	Method	Linear range (μM)	Detection limit (μM)	Ref.
Mn-complex-SWCNTs	Amperometry	1–1500	0.2	[3]
$[PFeW_{11}O_{39}]^{4-}$ polyoxoanion	Amperometry	10–200	7.4	[11]
AgNPs/PMES	Amperometry	0.6–540	0.18	[13]
Nanonickel oxide/thionine	Amperometry	5–20000	1.67	[19]
Nanonickel oxide/celestine blue	Amperometry	1–10000	0.37	[19]
Nano-TiO_2/DNA/thionin	Amperometry	50–22300	50	[30]
n-octylpyridinum Hexafluorophosphate	Amperometry	20–800	12	[32]
RB-MWCNT-GCE	Amperometry	0.99–2.8 × 10, 2.8 × 10–5.1 × 10^2 5.1 × 10^2–1.8 × 10^3	0.27	This work

AgNPs/PMES = silver nanoparticles/poly(2–(N–morpholine) ethane sulfonic acid); ERGO-Ag nanocomposite = electrochemically reduced graphene oxide (ERGO)-silver nanoparticle hybrid film; Mn–complex–SWCNTs = single wall carbon nanotubes and phenazine derivative of Mn–complex; PB/Pd–Al = aluminum electrode plated by thin layer metallic palladium and modified by Prussian blue; RB-MWCNT-GCE = reactive blue multiwalled carbon nanotubes modified glassy carbon electrode.

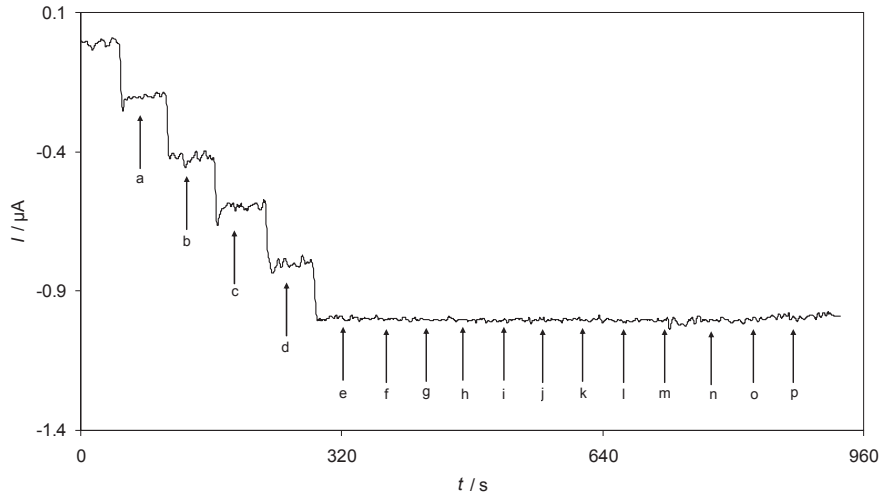

Fig. 7 – Amperometric responses at a rotating reactive blue 19 multiwalled carbon nanotube-modified glassy carbon electrode (rotation speed 2000 rpm) held at −300 mV in buffer solution (pH = 7) for successive addition of H_2O_2 (a–e, 20–220μM) and 1mM of (f) ascorbic acid, (g) uric acid, (h) glucose, (i) dopamine, (j) oxalic acid, (k) $NaNO_3$, (l) $Mg(NO_3)_2$, (m) KCl, (n) KI, (○) $NaNO_2$ and (p) Na_2SO_4.

inset B), from whose slope and using the Cottrell equation [25] a diffusion coefficient was calculated: 2.34×10^{-6} cm^2/s.

3.3. *Amperometric determination of H_2O_2*

Amperometry was used to determine the linear ranges and the detection limit of H_2O_2 at RB-MWCNT-GCE. The use of amperometry was based on the fact that it has a much higher current sensitivity than cyclic voltammetry. Fig. 6 shows the amperograms obtained for a rotating RB-MWCNT-GCE (rotation speed 2000 rpm), under conditions where the potential was held at −300 mV in a 0.1M phosphate buffer solution (pH 7.0) containing different concentrations (0.99–1.8mM) of H_2O_2.

The insets shown in Fig. 6 demonstrate the linear relationship of the electrocatalytic current vs. H_2O_2 concentration in the three linear ranges: (A) 0.99–28μM; (B) 28–510μM; and (C) 0.51–1.8mM. The decrease of sensitivity (slope) in the second and third linear range (higher analyte concentrations) is likely to be due to electrode surface pollution.

According to the method mentioned in reference [34], the lower detection limit, C_m, was found to be 0.27μM using the equation $C_m = 3s_{bl}/m$, where s_{bl} is the standard deviation of the blank response which is obtained from 14 replicate measurements of the blank solution (0.00077 μA) and m is the slope of the calibration plot (0.0086 μA/μM). Moreover, the limit of quantitation was calculated to be 0.9μM by limit of quantitation $= 10s_{bl}/m$ [34]. The average amperometric peak current and the precision estimated in terms of the coefficient of variation for repeated measurements ($n = 10$) of 15.0μM H_2O_2 at RB-MWCNT-GCE were 0.167 ± 0.005 μA and 3.02% respectively. It indicated that the sensor possessed good reproducibility. Also the stability of RB-MWCNT-GCE under working conditions was investigated in the presence of 100.0μM of H_2O_2. Inset D of Fig. 6 indicates the response stability of RB-MWCNT-GCE to 100.0μM of H_2O_2 solution during 2900 seconds. As shown, the amperometric current of H_2O_2 reduction remained almost constant during the experiment. In Table 3, some of the response characteristics obtained for H_2O_2 in this study are compared to those previously reported by others [3,11,13,19,30,32]. As can be seen, the responses of the proposed modified electrode are superior in some cases as compared to the previously reported modified electrodes.

Table 4 – Determination and recovery of H_2O_2 concentration in three fruit juice samples using reactive blue multiwalled carbon nanotube-modified glassy carbon electrode.

Samples	Added (μM)	Found[a] (μM)	RSD (%)	Recovery %
Apple juice	–	Not detected	–	–
	10.0	10.3	2.7	103
	20.0	19.5	2.2	97.5
Orange juice	–	Not detected	–	–
	8.0	8.2	2.5	102.5
	16.0	15.7	2.9	98.1
Banana juice	–	Not detected	–	–
	12.0	12.4	2.8	103.3
	24.0	23.5	2.1	97.9

RSD = Relative Standard Deviation.
[a] Three replicate measurements were made on the same samples. Detection limit = 0.27μM.

3.4. *Interference study*

An important problem in determining H_2O_2 is the effect of potential interfering ions. A survey on the influence of various substances as potential interfering compounds on the H_2O_2 determination under optimum conditions at the RB-MWCNT-GCE surface was done. Fig. 7 shows the amperometric response of modified electrode during addition of 20–220μM of H_2O_2 and different interferences to buffer solution (pH 7). As

illustrated, nearly all compounds such as ascorbic acid, uric acid, glucose, dopamine, oxalic acid, $NaNO_3$, $Mg(NO_3)_2$, KCl, KI, $NaNO_2$, and Na_2SO_4 do not interfere when present in 1.0 mM concentration. The sensor response toward H_2O_2 before and after interference injection is the same. The results indicate that H_2O_2 recovery was almost quantitative in the presence of an excess amount of possible interfering species at this sensor.

3.5. *Analysis of real samples*

Sometimes, for the aseptic packaging of fruit juices, H_2O_2 is used as a chemical agent for sterilization. However, the H_2O_2 residues in higher concentration are skin irritants and may affect the human health. Therefore, determination of H_2O_2 in fruit juices is important. The maximum level of H_2O_2 residual allowed in the aseptic packaging in accordance with US Food and Drug Administration (21 CFR 178.1005) is 0.5 ppm (14.7μM). Since the lower linear range of the proposed sensor is 0.99–28.0μM, this sensor can be applied for determination of H_2O_2 in aseptic packaging.

From the results, it is apparent that RB-MWCNT-GCE possesses a high sensitivity and a good detecting capability to determine H_2O_2 in real samples. In order to test its practical application, the modified electrode was used to determine H_2O_2 in three fruit juice samples. As the electrochemical techniques are able to determine H_2O_2 without pretreatment, therefore the fruit juice samples were directly inserted to the experimental cell. To do the experiment, 2 μL of a fruit juice sample were diluted down to 10 μL with a 0.1 M phosphate buffer solution (pH 7.0). Then, known amounts of H_2O_2 were added, and their recoveries were determined using amperometric measurements. The results in Table 4 indicate that the Percentage of relative standard deviation (RSD%) and the recovery rates of the spiked samples are acceptable. Thus, RB-MWCNT-GCE can be efficiently used for H_2O_2 determination in different fruit juice samples. It is concluded that the matrix of fruit juice samples does not interfere in determination of H_2O_2 at the proposed sensor.

3.6. *Conclusions*

This paper demonstrates the construction of an RB-MWCNT-GCE and its application in determination of H_2O_2. The results of the study show that RB can be immobilized easily at the surface of MWCNT-modified GCE. Kinetic parameters such as the catalytic rate constant, k_s, transfer coefficient, α, the number of electrons involved in the rate determining step, n_α, and the overall number of electrons involved in the catalytic reduction of H_2O_2 at the modified electrode surface have also been determined using cyclic voltammetry. The diffusion coefficient of H_2O_2 has been found to be 2.34×10^{-6} cm^2/s for experimental conditions using chronoamperometric results. RB–MWCNT–GCE exhibits three wide linear ranges of 0.99–28μM, 28–510μM, and 0.51–1.8mM for H_2O_2 determination by amperometry. The lower detection limit of H_2O_2 at the modified electrode is 0.27μM. Also, amperometry can be used as an analytical method for H_2O_2 determination in real samples.

Conflicts of interest

The authors declare no conflicts of interest.

REFERENCES

[1] Farah AM, Shooto ND, Thema FT, Modise JS, Dikio ED. Fabrication of Prussian blue/multi-walled carbon nanotubes modified glassy carbon electrode for electrochemical detection of hydrogen peroxide. Int J Electrochem Sci 2012;7:4302–13.

[2] Salimi A, Mahdioun M, Noorbakhsh A, Abdolmaleki A, Ghavami RA. Novel non-enzymatic hydrogen peroxide sensor based on single walled carbon nanotubes–manganese complex modified glassy carbon electrode. Electrochim Acta 2011;56:3387–94.

[3] Song MJ, Hwang SW, Whang D. Amperometric hydrogen peroxide biosensor based on a modified gold electrode with silver nanowires. J Appl Electrochem 2010;40:2099–105.

[4] Taniai T, Sakuragawa A, Okutani T. Fluorometric determination of hydrogen peroxide in natural water samples by flow injection analysis with a reaction column of peroxidase immobilized onto chitosan beads. Anal Sci 1999;15:1077–82.

[5] Hurdis EC, Romeyn H. Accuracy of determination of hydrogen peroxide by cerate oxidimetry. Anal Chem 1954;26:320–5.

[6] Rocha FRP, Torralba ER, Reis BF, Rubio AM, Guardia MA. portable and low cost equipment for flow injection chemiluminescence measurements. Talanta 2005;67:673–7.

[7] Matos C, Coelho EO, De Souza CF, Guedes FA, Matos MA. Peroxidase immobilized on Amberlite IRA-743 resin for on-line spectrophotometric detection of hydrogen peroxide in rainwater. Talanta 2006;69:1208–14.

[8] Kok GL, Holler TP, Lopez MB, Nachtrieb HA, Yuan M. Chemiluminescent method for determination of hydrogen peroxide in the ambient atmosphere. Environ Sci Technol 1978;12:1072–6.

[9] Mashazi PN, Ozoemena KI, Nyokong T. Tetracarboxylic acid cobalt phthalocyanine SAM on gold: potential applications as amperometric sensor for H_2O_2 and fabrication of glucose biosensor. Electrochim Acta 2006;52:177–86.

[10] Thenmozhi K, Narayanan SS. Electrochemical sensor for H_2O_2 based on thionin immobilized 3-aminopropyltrimethoxy silane derived sol–gel thin film electrode. Sens Actuators B 2007;125:195–201.

[11] Hamidi H, Shams E, Yadollahi B, Kabiri Esfahani F. Fabrication of carbon paste electrode containing $[PFeW_{11}O_{39}]^{4-}$ polyoxoanion supported on modified amorphous silica gel and its electrocatalytic activity for H_2O_2 reduction. Electrochim Acta 2009;54:3495–500.

[12] Majidi M, Pournaghi-Azar MH, Saadatirad A, Alipour E. Simple and rapid amperometric monitoring of hydrogen peroxide at hemoglobin-modified pencil lead electrode as a novel biosensor: application to the analysis of honey sample. Food Anal Methods 2015;8:1067–77.

[13] Zhang K, Zhang N, Xu J, Wang H, Wang C, Shi H, et al. Silver nanoparticles/poly(2-(N-morpholine) ethane sulfonic acid) modified electrode for electrocatalytic sensing of hydrogen peroxide. J Appl Electrochem 2011;41:1419–23.

[14] Kalantar-Dehnavi A, Rezaei-Zarchi S, Mazaheri Gh, Negahdary M, Malekzadeh R, Mazdapour M. Designing a H_2O_2 Biosensor by using of modified graphite electrode with

nano-composite of nafion-nile blue-peroxidase enzyme. Eur J Exp Biol 2012;2:672–82.
[15] Saber-Tehrani M, Pourhabib A, Husain SW, Arvand M. A simple and efficient electrochemical sensor for nitrite determination in food samples based on Pt nanoparticles distributed poly(2-aminothiophenol) modified electrode. Food Anal Methods 2013;6:1300–7.
[16] Chandran S, Lonappan LA, Thomas D, Jos T, Girish K, Kumar KG. Development of an electrochemical sensor for the determination of amaranth: a synthetic dye in soft drinks. Food Anal Methods 2014;7:741–6.
[17] Rasheed Z, Vikraman AE, Thomas D, Jagan JS, Kumar KG. Carbon-nanotube-based sensor for the determination of butylated hydroxyanisole in food samples. Food Anal Methods 2015;8:213–21.
[18] Raoof JB, Teymoori N, Khalilzadeh MA. ZnO nanoparticle ionic liquids carbon paste electrode as a voltammetric sensor for determination of Sudan I in the presence of vitamin B6 in food samples. Food Anal Methods 2015;8:885–92.
[19] Noorbakhsh A, Salimi A. Amperometric detection of hydrogen peroxide at nano-nickel oxide/thionine and celestine blue nanocomposite-modified glassy carbon electrodes. Electrochim Acta 2009;54:6312–21.
[20] Vianello F, Zennaro L, Rigo AA. Coulometric biosensor to determine hydrogen peroxide using a monomolecular layer of horseradish peroxidase immobilized on a glass surface. Biosens Bioelectron 2007;22:2694–9.
[21] Chen X, Chen Z, Zh J, Xu C, Yan W, Yao C. A novel H_2O_2 amperometric biosensor based on gold nanoparticles/self-doped polyaniline nanofibers. Bioelectrochemistry 2011;82:87–94.
[22] Zare HR, Nasirizadeh N, Mazloum–Ardakani M. Electrochemical properties of a tetrabromo-p-benzoquinone modified carbon paste electrode. Application to the simultaneous determination of ascorbic acid, dopamine and uric acid. J Electroanl Chem 2005;577:25–33.
[23] Nasirizadeh N, Shekari Z, Zare HR, Makarem S. Electrocatalytic determination of dopamine in the presence of uric acid using an indenedione derivative and multiwall carbon nanotubes spiked in carbon paste electrode. Mater Sci Eng C 2013;33:1491–7.
[24] Nasirizadeh N, Shekari Z, Zare HR, Shishehbore MR, Fakhari AR, Ahmar H. Electrosynthesis of an imidazole derivative and its application as a bifunctional electrocatalyst for simultaneous determination of ascorbic acid, adrenaline, acetaminophen, and tryptophan at a multi-wall carbon nanotubes modified electrode surface. Biosen Bioelectron 2013;41:608–14.
[25] Bard AJ, Falkner LR. Electrochemical methods: fundamentals and applications. NewYork: Wiley; 2001.
[26] Laviron E. General expression of the linear potential sweep voltammogram in the case of diffusionless electrochemical systems. J Electroanal Chem 1979;101:19–28.
[27] Zare HR, Nasirizadeh N, Chatraei F, Makarem S. Electrochemical behavior of an indenedione derivative electrodeposited on a renewable sol–gel derived carbon ceramic electrode modified with multi-wall carbon nanotubes: application for electrocatalytic determination of hydrazine. Electrochim Acta 2009;54:2828–36.
[28] Zare HR, Shekari Z, Nasirizadeh N, Jafari AA. Fabrication, electrochemical characteristics and electrocatalytic activity of 4-((2-hydroxyphenylimino)methyl)benzene-1,2-diol electrodeposited on a carbon nanotube modified glassy carbon electrode as a hydrazine sensor. Catal Sci Technol 2012;2:2492–501.
[29] Miller JN, Miller JC. Statistics and chemometrics for analytical chemistry. 4th ed. London: Pearson Education Ltd; 2000.
[30] Lo PH, Kumar SA, Chen SM. Amperometric determination of H_2O_2 at nano-TiO_2/DNA/thionin nanocomposite modified electrode. Colloids Surfaces B 2008;66:266–73.
[31] Bai YH, Du Y, Xu JJ, Chen HY. Choline biosensors based on a bi-electrocatalytic property of MnO_2 nanoparticles modified electrodes to H_2O_2. Electrochem Commun 2007;9:2611–6.
[32] Haghighi B, Hamidi H, Gorton L. Formation of a robust and stable film comprising ionic liquid and polyoxometalate on glassy carbon electrode modified with multiwalled carbon nanotubes: toward sensitive and fast detection of hydrogen peroxide and iodate. Electrochim Acta 2010;55:4750–7.
[33] Andrieux CP, Saveant JM. Heterogeneous (chemically modified electrodes, polymer electrodes) vs. homogeneous catalysis of electrochemical reactions. J Electroanal Chem 1978;93:163–8.
[34] Skoog DA, Holler FJ, Nieman TA. Principles of Instrumental Analysis. 5th ed. London: Saunders College Publishing; 1998.